Delta J. Sci. 20 (1) 1996, 92-103

RADIOACTIVE AND ELECTROMAGNETIC LOGGING STUDIES MAYOS HORMUS-3 WELL, RED SEA, EGYPT

BY

Abou Shagar, S. M.

Received: 14 - 6 - 1995

ABSTRACT

Both natural gamma ray spectroscopy (NGS) and electromagnetic propagation tools are used in order to identify the dominant cly minerals and to determine the electromagnetic porosity. The data collected from one well located at the southern part of the Gulf of Suez area is selected for carrying out this study. Clay mineral type can be best identified from the NGS tool. Electromagnetic porosities can be best determined from both electromagnetic wave propagation time and their attenuation. The identified clay minerals are mainly represented by montmorillonite and illite. These two clay minerals are distributed along both the Belayem and Kareem Formation of the Middle Miocene age. Electromagnetic porosities range between 0.18 and 0.60. The interpreted environment that can be detected from this study is shallow evironment of alkaline type.

INTRODUCTION

Radioactive logs are either natural or artificial. Natural logs are represented by two types of recording (traditional gamma ray and gamma ray spectrometry NGS). Nearly all the gamma radiation is emitted by the radioactive potasium isotope (K^{40}), beside other radioactive elements such as U^{238} and Th^{232} (Cox, 1979 and Schlumberger, 1989). In general gamma rays experience successive compton-scattering collisions with atoms of the formation material causing loss of energy with each collision. When enough energy is lost the gamma ray is absorped by means of photoelectric effect. The rate of absorption varies with formation density, where the less dense formation the more radioactive and vice versa:

$$GR = (\sum \rho_i V_i A_i)/\rho_b \quad \text{,(Schlumberger,1989)}$$

where

GR: gamma ray intensity.

ρ_i: density of the radioactive mineral.

V_i: bulk volume factor of the mineral.

A_i: proportionality factor corresponding to the radioactivity of the mineral.

ρ_b: formation bulk density.

The NGS log measures the natural radioactivity of the formation represented by a number of gamma ray of different energy levels. This method permits the determination of the concentration of K^{40}, U^{238} and Th^{232} with half life of $1.3x10^9$, $4.4x10^9$and $1.4x10^{10}$years, respetively. K^{40} is a direct product of Ca^{40} and Ar^{40} as a result of decay and electron capture, respectively. The radioactive decay of both U^{238} and Th^{232} produces Pb^{206} and Pb^{208}, respectively. Figure (1) shows the gamma ray emission spectra of the different radioactive elements. Concerning the shale deposits for which their mineral constituents are detectable using the NGS tool the propable concentration of U, Th and K are 3.8, 12 and 28000ppm, respectively. Brownlow (1979), Baldwin et al. (1980) and Quirein et al. (1982) studied the application of the NGS for complex lithology identification. The cross plot method is used to define the clay type, Schlumberger (1989).

Most resistivity methods depend on water salinity, so some problems are faced in determining the medium porosity. A method that is relatively less dependent upon water salinity has long been needed to determine water saturation from porosity. The measurement of the dielectric constant is one of these methods. Table (1) shows the dielectric constants of some rocks and fluids. From this table it is clear that most minerals is sedimentary rocks have values less than 8 except water, where it exceeds the value 50. For this reason this method is primarily a function of water-filled

porosity. According to Maxwell's equation electromagnetic propagation can be expressed as:

$$\gamma = \alpha + j\,ß$$

$$\omega\,\mu\,c = 2\,\alpha\,ß$$

where:

γ: is the electromagnetic wave propagation

α: is the attenuation of the wave

j: current density

ß: is the phase shift

μ: is the magnetic permeability

ω: is the wave angular velocity

c: is the conductivity

Based on the depth of investigation two tools for the electromagnetic well logging have been designed (Schlumberger, 1989); these are the shallow (EPT) and the deep (DPT) investigations. The results are represented by electromagnetic wave attenuation (EATT) in db/m and propagation time (tpl) in nanos./m.

Various interpretation methods of the electromagnetic propagation tool are known (Schlumberger, 1989). The complex refractive index method (CRIM) is an iterative process by which the water-filled porosity and the saturation water electromagnetic wave propagation are determined. The complex time average model (CTA) can be also used for the determination of the electromagnetic porosity (ΦEPT). The well known weight average equation that used in many fields can be applied here, where it takes the form:

$$\gamma^* = \varphi\ \gamma f + (1-\varphi)\gamma ma$$

γ^* :total electromagnetic wave propagation

$\varphi\,\gamma f$:the electromagnetic wave propagation in the pore fluid .

γma : the electromagnetic wave propagation in the rock matrix.

φ : the porosity

Both propagation time and attenuation can be used for the (ϕEPT) calculation. Before using this technique, the measured values of propagation time (tpl) and attenuation (ϕEPT) must be corrected for the propagation phenomena of geometrical spreading and scattering (Schlumberger, 1989). The calculated electromagnetic porosities (ϕEPT) are recorded on one of the log tracks. Comparison of ϕEPT and porosities measured by other logging tools (Neutron, Sonic and density) allows a quicklook determination of the water saturation specially in the flushed zone. It should be mentioned here that porosity will be the same as the total porosity in water bearing zones. In hydrocarbon bearing intervals it will be less than the total porosity. In gas zones both and neutron porosity are the same because of the excavation effect on the neutron measurement. Fig. (2) shows porosity ranges in the different gas, oil, and water bearing zones.

Data analysis and Interpretation

To apply both NGS and EPT logging tools a well located at the southern part of the Gulf of Suez at the junction with the Red Sea (Myos Hormas-3) is selected (Fig. 3) The subsurface geology in this area as described by Barakat (1984), can be summarized as follows:

Miocene section is the most dominating one where it ranges in thickness between 528 and 4628m. Miocene section is divided into early, Middle and Middle-late Miocene. The early and a part of the middle Miocene is formed of Nukhul, Rudies, Kareem and Belayem Formations from base to top, respectively. The general lithological composition is of clastic type (shale and sandstone). The upper part of Middle Miocene and the whole Upper Miocene are formed of South Gharib and Zeit Formations where they mostly formed of evaporites. A main surface of unconformity between Paleocene/Miocene is present where Oligocene is missed. Five formations in

the study well are reached by drilling. These formations, their thicknesses and lithological associations are represented in Table (2).

Table (2): The formations encountered in Myos Hormos-3 well and their equivalent depths, thicknesses and lithology.

Formation	Depth (M)	Thickness (M)	Shale%	S.S%	L.S%	Salt%	Anhydrite%
Zeit	287	80	37.5	-	12.5	-	50
South Gh.	367	886	6.3	-	-	55.3	38.4
Belayem	1253	183	35.7	11 9	-	-	52.4
Kareem	1436	170	88.2	-	-	-	12.8
Rudies	1633	310	88.1	-	12.9	-	-
Nukhul	1943						

N.B. : S.S. = Sandstone, L.S. = Limestone.

It should be mentioed here that both NGS tool for clay type identification and the electromagnetic method for electromagnetic porosity determination can not be used for Zeit and South Gharib Formations for their lithological characteristics (evaporite types). Fourteen depth intervals extendig from 1295m to 1943m are interpreted. Figs 4 and 5 show parts of both NGS and EPT logs belonging to the study intervals. The corresponding clay type mineralogy and ϕEPT are listed in table 3.

Table (3): Depth intervals and their eqivalent information as deuced from the NGS and Electromagnetic propagation.

Depth Int. (M)	Thickness (M)	Th (ppm)	K %	ϕEPT (p.u.)	Clay type
1295-1301	6	4	2.8	0.52	Montmorillonite
1301-1311	10	6	1.2	0.52	Montmorillonite
1372-1396	24	6	1	0.50	Montmorillonite
1418-1423	5	7	1	0.55	Montmorillonite
1533-1567	34	8	1	0.60	Montmorillonite
1594-1653	59	6	1	0.60	Montmorillonite
1665-1667	2	4	1	0.52	Montmorillonite
1683-1688	5	5	1	0.33	Montmorillonite
1688-1696	11	7	1	0.50	Montmorillonite
1710-1725	15	7	1	0.60	Montmorillonite
1734-1741	7	7	1	0.30	Montmorillonite
1744-1756	12	4	1	0.18	Montmorillonite
1817-1847	30	5	3	0.40	Illite
1887-1890	3	6	2	0.21	Illite

Conclusions

Natural gamma ray spectroscopy is used to identify the shaly intervals and its caly mineral content. Both montmorillonite and illite are detected at some intervals in the four study formations (Belayem, Kareem, Rudies and Nukhul). Electromagnetic porosities are calculated and range between 18-60%.

REFERENCES

Baldwin, J.L., Quirein, J.A. and Serra, O. 1980: Theory and practical application of NGS: Trans. SPWLA Annual Logging Symposium.

Barakat, H. and Miller, P. 1984: Geology and petroleum exploration, Safaga Concession, Northern Red Sea, Egypt, EGC, pp. 191-214.

Brownlow, A.H. 1979: Geochemistry: Prentice-HAll, INC, Englewood Cliffs.

Cox, J.W. and Raymer, L.L. 1976: The effect of potasium salt muds on gamma ray and S.P. measurements: Trans. SPWLA, Annual Logging Symposium.

Quirein, J.A., Gardner, J.S. and Watson, J.T. 1982: Combined Natural Gamma Ray spectral litho-density measurements applied to complex lithologies: SPE Annual Technical Conference, SPE 11143

Schlumberger, 1989: Log Interpretation Principles/Applications-Houston

Table (1): Relative dielectric constants and propagation times for common rocks, minerals and fluids, (Schlumberger, 1989).

Mineral	Relative Dielectric Constant	Propagation time t_{pl}(ns/m)
Sandstone	4.65	7.2
Dolomite	6.8	8.7
Limestone	7.5-9.2	9.1-10.2
Anhydrite	6.35	8.4
Halite	5.6-6.35	7.9-8.4
Gypsum	4.16	6.8
Dry colloids	5.76	8
Shate	5.25	7.45-16.6
Oil	2-2.4	4.7-5.2
Gas	1	3.3
Water	56-80	25-30
Fresh water	78.3	29.5

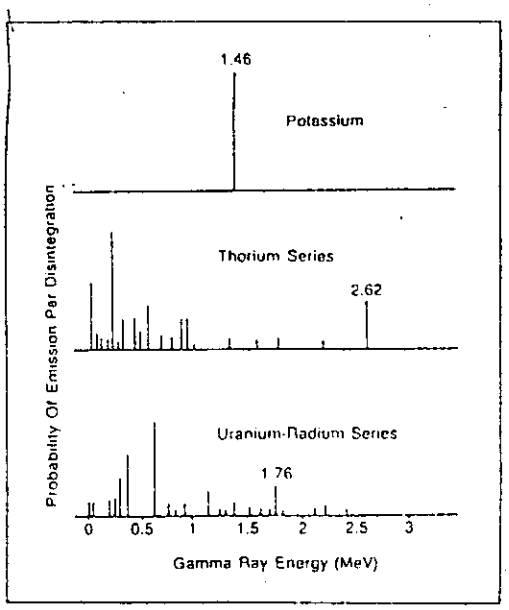

Fig. (1)-Gamma ray emission spectra of radioactive minerals, (Schlumberger, 1989).

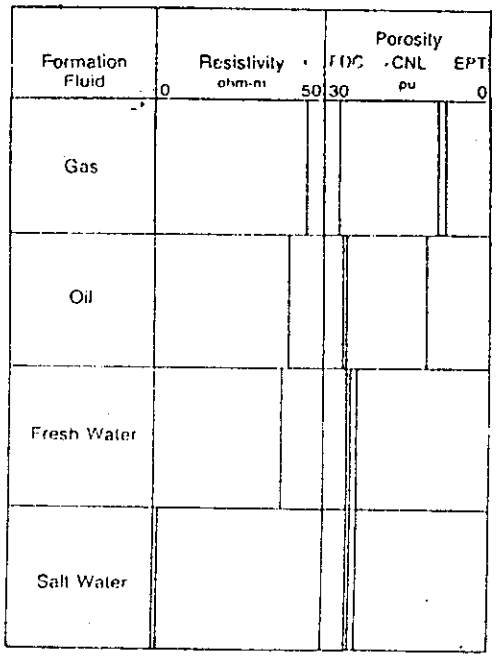

Fig. (2)-Variation of log readings in water and hydrocarbons, (Schlumberger, 1989).

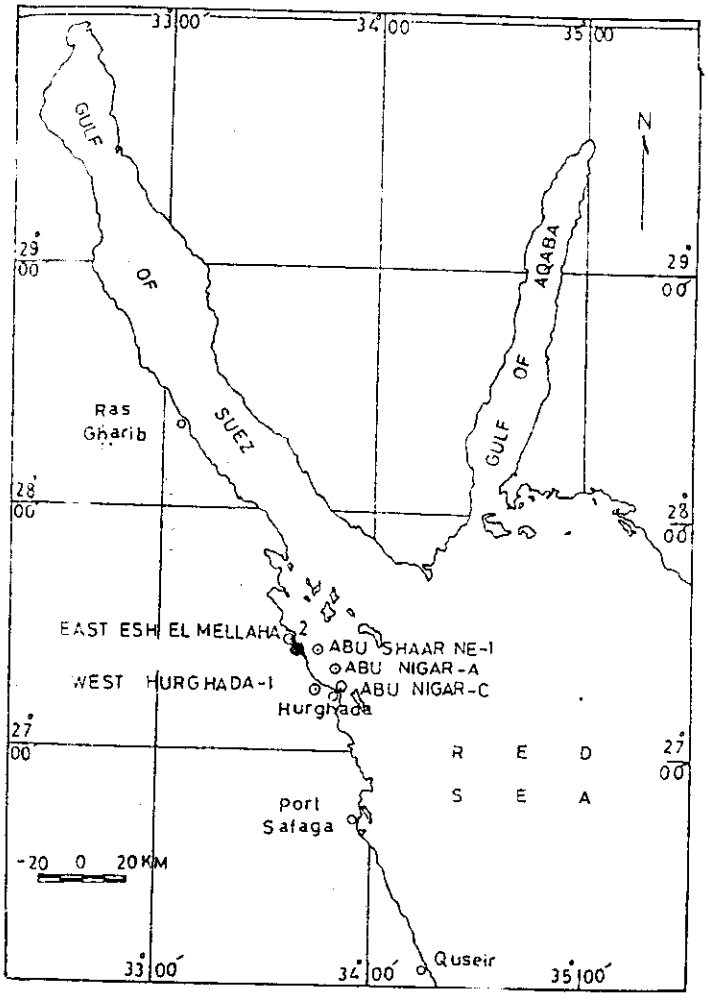

Fig. (3)-Southern part of the Gulf of Suez at the junction with the Red Sea (Myos Hormos-3).

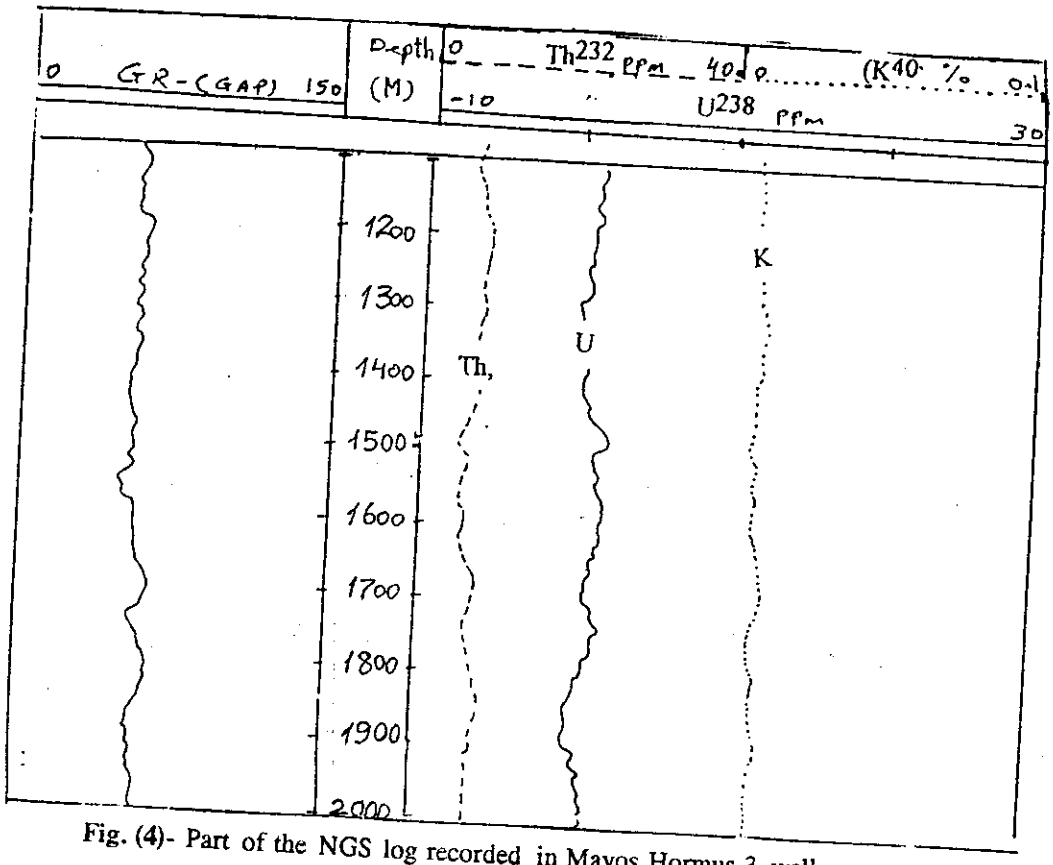

Fig. (4)- Part of the NGS log recorded in Mayos Hormus-3 well.

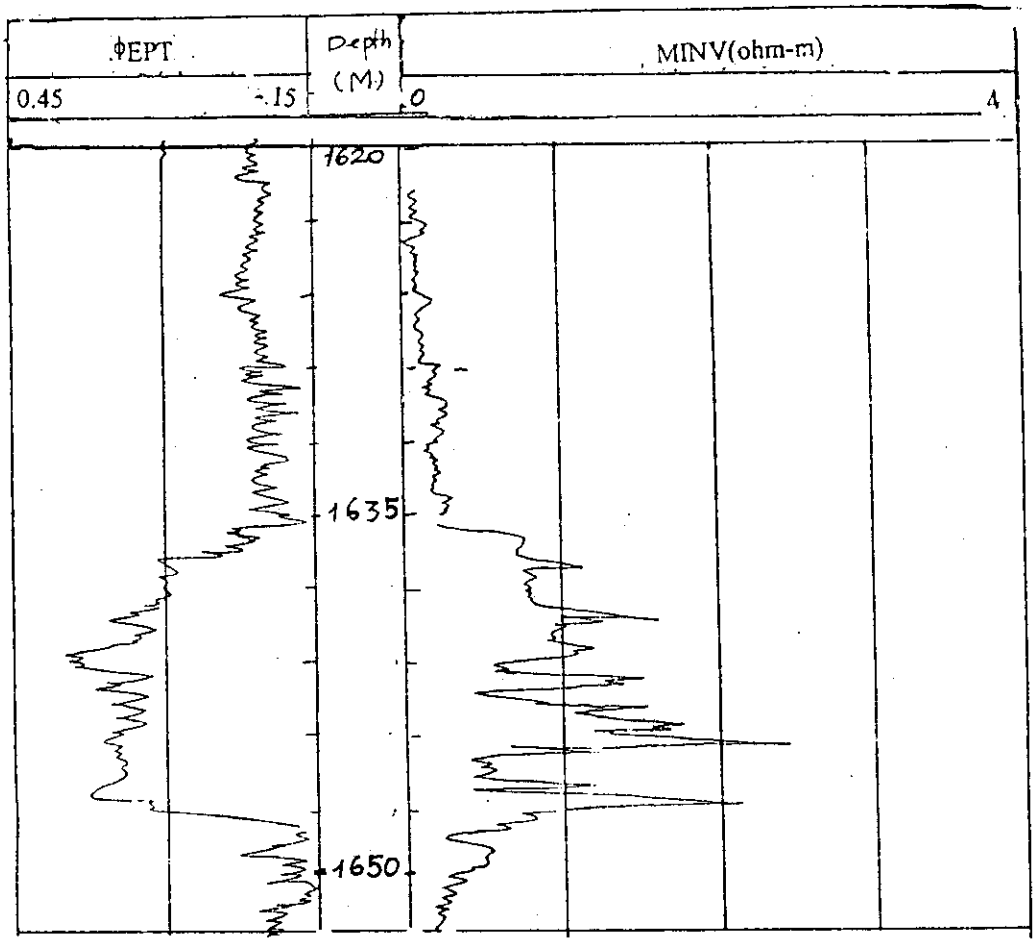

Fig. (5)- Part of the electromagnetic log recorded in Mayous Hormus-3 well.

Delta J. Sci. 20 (1) 1996

دراسات تسجيلات الآبار الإشعاعيه والكهرومغناطيسيه - ميوس هرمز -٣- البحر الأحمر - مصر

السيدة محمد السيد أبو شجار

يتناول البحث التعرف على معادن الطفله الموجوده فى صخور الميوسين لتكوينات بلاعيم ، كريم ونخل لبئر ميوس هرمز ٣ وقد تم استخدام طيف أشعة جاما والكهرومغناطيسيه ومن تحليل تلك السجلات أمكن التعرف على معادن المونتموربلونيت والاليت وكذلك تم حساب المساميه من الأشعه الكهرومغناطيسيه وكانت مابين ١٨-٦٠٪. كما أن البيئة الترسيبية كانت ضحلة ومن النوع القلوى .